Computers and Geotechnics 78 (2016) 88–98

Contents lists available at ScienceDirect

Computers and Geotechnics

journal homepage: www.elsevier.com/locate/compgeo

Research Paper

Investigation of retrogressive and progressive slope failure mechanisms using the material point method

B. Wang, P.J. Vardon *, M.A. Hicks

Geo-Engineering Section, Faculty of Civil Engineering and Geosciences, Delft University of Technology, The Netherlands

ARTICLE INFO

Article history:
Received 27 October 2015
Received in revised form 10 March 2016
Accepted 27 April 2016

Keywords:
Dynamics
Failure mechanism
Material point method
Retrogressive failure
Slope stability

ABSTRACT

Retrogressive and progressive slope failures are a dynamic process, in the sense that they involve a progressively changing scenario. This paper uses the contemporary material point method (MPM), to provide a view of how such failures develop. Two main scenarios are presented: (a) a relatively small slope, which, when subjected to an initial failure, is steepened, leading to the initiation of further failures retrogressing backwards; and (b) a long slope, where an initial perturbation (e.g. an excavation) triggers a series of failures that can retrogressively move up-slope.

1. Introduction

Informally, "a movement of a mass of rock, earth or debris down a slope" is defined as a landslide [1]. Based on the type of material (e.g. rock, soil) and the mode of the movement (e.g. falls, slides) involved, various types of landslides have been identified [2–4]. The corresponding failure mechanisms, identified mostly through the back analysis of case histories, are also diverse and complicated, due to the interactions of adjacent sliding bodies [4]. A number of related descriptions have been summarised [3], such as advancing, enlarging, progressive or retrogressive.

If an initial slide occurs and the material in the failure flows away, which is usually caused by a high degree of strength loss, a steep main scarp will usually be formed and therefore support for the remaining soil will be removed. This can result in another failure, termed a retrogressive failure. This process can repeat itself in a multiple-retrogressive fashion, and can result in a bigger landslide. In some slopes, such strength loss does not occur almost instantaneously, but is associated with the magnitude of shear strain, so that the rupture surface propagates through the soil profile over time. In this case, the term "progressive" is used. Reported cases include the retrogressive failures of cemented sensitive clays in the Ottawa–St. Lawrence Lowlands [5]; retrogressive landslide complexes in the Boone valley in the French Alps [6]; and the progressive failures of observed landslides in Scandinavia and eastern Canada [7]. The recent Oso landslide in Washington was observed to have multi-rotational retrogressive failures in parts and large translational slides in the longer slopes [8].

Investigations into the conditions triggering landslides have also been initiated [9–13], in order to find efficient ways to mitigate landslides along with their significant impacts. Common destabilising factors include rainfall infiltration, water level rise, and earthquakes. Site investigations on real slope failures provide very valuable information; however, the intervals between individual failures in a larger slide can sometimes amount to some tens of years [14]. In most cases of real slope failures, instrumentation of the failure and material characterisation are not undertaken. Hence, for helping to investigate slope failure conditions in a time efficient way, numerical modelling shows certain advantages. A recent publication [15] compares material point method (MPM) simulation with two real cases, although the only comparison is the final failed slope configuration; hence there is no comparison with any failure or propagation mechanisms, e.g. rotational or progressive failures.

This paper presents a numerical framework which is able to simulate the whole slope failure process, from initiation, through failure propagation, to the final equilibrium configuration. For convenience in benchmarking this technique, some idealised assumptions are made, but these can easily be changed for more site specific analyses. The simplifying assumptions are: (a) the flow material is a clay idealised by a linear elastic, cohesion strain softening Von Mises model; (b) the slope is assumed to be initially

* Corresponding author.
E-mail addresses: B.Wang@tudelft.nl (B. Wang), P.J.Vardon@tudelft.nl (P.J. Vardon), M.A.Hicks@tudelft.nl (M.A. Hicks).

http://dx.doi.org/10.1016/j.compgeo.2016.04.016
0266-352X/

unstable under the in-situ stress condition, so that self-weight is the trigger for the slope failure rather than any of the factors mentioned above; (c) no pore pressure changes are simulated. Hence, a simple total stress approach is adopted in this paper, with the aim of giving a clear (albeit simplified) picture of some of the main geometric features of slope failure mechanisms in cohesive soils; that is, as a prequel to future investigations involving more realistic material and triggering scenarios. The emphasis here is to reproduce commonly seen clay-type slope failures [5–7] (e.g. rotational and translational slides), and to interpret the failure mechanisms within the proposed framework; that is, to explain the observed translational and rotational slides through the concepts of retrogressive and progressive failure. Comparison of simulations to field cases is beyond the scope of this investigation.

For modelling slope instability, traditional numerical tools such as the finite element method are often limited in their applicability to problems involving large deformations, due to potential excessive mesh distortions that can occur in such cases. This can give an incomplete description of failure, in that the initial slip is considered and the ongoing sliding failure is ignored. That is, continual changes in geometry cannot easily be simulated without extensive re-meshing. However, by using the implicit material point method (IMPM) [16] coupled with a cohesive softening (Von Mises type) constitutive model, the process of retrogressive failure in an undrained soft clay under self-weight loading is possible, as will be demonstrated herein. For this purpose, two types of slope are analysed, which, for convenience, are called "short slope" (slope height = 5.0 m) and "long slope" (down-slope length ≈ 25.0 m). The factors influencing the post-failure and retrogressive failure behaviours of the two slopes have been investigated. For the long slope, different slope angles are considered, to investigate the link between slope geometry and the various failure mechanism categories.

2. Implicit material point method

MPM has proven to be a useful finite element method (FEM) variant for simulating large-strain problems in geotechnical applications [17–20], with the material points representing the continuum being capable of moving through a background mesh, thereby removing the limitation of excessive mesh distortions that can occur in FEM. The implicit material point method (IMPM) here refers to an MPM framework where the governing equation is solved implicitly, which can be used for both quasi-static and dynamic analyses. It addresses time step size limitations, which are an inherent problem in explicit dynamics, and can thus reduce the computational cost in many cases. The full details of IMPM can be found in Wang et al. [16], with the focus of this paper being retrogressive failure mechanisms. However, the essential features of the method and governing equations are briefly presented below.

The two major differences between MPM and FEM are that: (a) MPM uses two types of discretisation; and (b) within each computational cycle (i.e. loading/time step), the material points function as the integration points instead of traditional Gaussian points. The two types of discretisation, as shown in Fig. 1, are: (a) a background mesh, which is used for the computation and can be reset regularly to avoid the mesh distortions; and (b) a set of material points, which represent the material, store all the state variables and are allowed to move freely through the mesh. Hence no state variables are stored on the nodes, and a connectivity therefore needs to be set up between the material points and the background mesh. This is so that the information can be mapped to the background mesh before each loading/time step, for initialising the computation, and then mapped back to the material points after the loading/time step so that the background mesh can be reset.

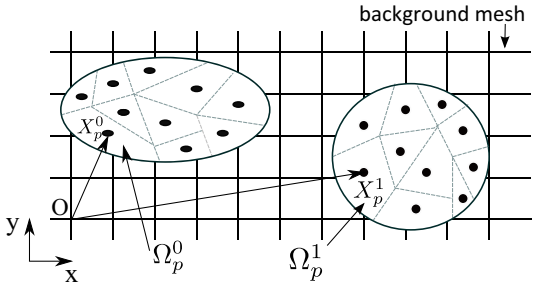

Fig. 1. Spatial discretisations in MPM, in which the superscript "0" represents the continuum initial state, and "1" stands for the deformed state; the background mesh is used for the computation step (after Sulsky et al. [21]).

2.1. Formulation

As in an updated Lagrangian FEM formulation, the equilibrium of the continuum at time $t+\Delta t$ is to be solved, by assuming that equilibrium has been attained at time t. Starting from the mass and momentum conservations at the continuum scale, and applying the principle of virtual displacement, followed by the use of the divergence theorem, the governing equation in the weak form at time $t+\Delta t$ is

$$\int_{V^{t+\Delta t}} \boldsymbol{\sigma}^{t+\Delta t} \cdot \nabla \cdot \delta \mathbf{u}^{t+\Delta t} dV = \int_{V^{t+\Delta t}} \mathbf{b}^{t+\Delta t} \cdot \delta \mathbf{u}^{t+\Delta t} dV + \int_{S^{t+\Delta t}} \boldsymbol{\tau}^{t+\Delta t} \cdot \delta \mathbf{u}^{t+\Delta t} dS \quad (1)$$

where $\boldsymbol{\sigma}$ is the Cauchy stress, $\mathbf{b}$ is the body force due to, for example, gravity, $\boldsymbol{\tau}$ denotes the prescribed part of the traction on the surface S, V is the volume of the body and $\delta\mathbf{u}$ represents the virtual displacement. For large deformation analysis, the Jaumann stress rate and velocity strain tensors have been adopted [22].

The integrals of the weak form are easily converted to the sums of quantities evaluated at the material points. Details can be found in Wang et al. [16] and Guilkey and Weiss [23]. The final equilibrium equation can then be expressed in matrix form as,

$$\mathbf{K}^t \Delta \mathbf{u} = \mathbf{R}^{t+\Delta t} - \mathbf{F}_{int}^t \quad (2)$$

where $\mathbf{K}^t = \mathbf{K}_L^t + \mathbf{K}_{NL}^t$ taking into account the large strain deformation, $\Delta\mathbf{u}$ is the vector of incremental nodal displacements, $\mathbf{R}^{t+\Delta t}$ is the external loading accounting for both traction and body loads on the continuum and $\mathbf{F}_{int}^t$ is the internal force.

As an example, the linear elastic stiffness at time t is expressed as,

$$\mathbf{K}_L^t = \sum_p \left(\mathbf{B}_L^{\mathrm{T}}(\mathbf{x}_p) \mathbf{C}_p \mathbf{B}_L(\mathbf{x}_p) \right) V_p \quad (3)$$

where $\mathbf{B}_L$ is the matrix of shape function spatial differentials, $\mathbf{C}_p$ is the stress–strain relationship which is traced on each individual material point, $\mathbf{x}_p$ are the coordinates of a material point, V_p is the volume associated with a material point, and subscript p refers to a material point. The non-linear part of the stiffness term is expressed in a similar manner [16].

A dynamic solution can be readily obtained by adding an inertial term in Eq. (2), to give

$$\mathbf{K}^t \Delta \mathbf{u} + \mathbf{M}^t \mathbf{a}^{t+\Delta t} = \mathbf{R}^{t+\Delta t} - \mathbf{F}_{int}^t \quad (4)$$

where $\mathbf{M}$ is the mass matrix and $\mathbf{a}$ is the acceleration. The following relationship between the kinetic variables is also assumed [24]:

$$\mathbf{v}^{t+\Delta t} = \mathbf{v}^t + [(1-\delta)\mathbf{a}^t + \delta \mathbf{a}^{t+\Delta t}] \Delta t \quad (5)$$

$$\mathbf{u}^{t+\Delta t} = \mathbf{u}^t + \mathbf{v}^t \Delta t + \left[\left(\frac{1}{2} - \alpha \right) \mathbf{a}^t + \alpha \mathbf{a}^{t+\Delta t} \right] \Delta t^2 \quad (6)$$